Published OnlineFirst August 30, 2017; DOI: 10.1158/0008-5472.CAN-17-0707

Microenvironment and Immunology

Cancer Research

CD73 Promotes Resistance to HER2/ErbB2 Antibody Therapy

Martin Turcotte[1,2,3], David Allard[1,2,3], Deepak Mittal[4,5], Yacine Bareche[6,7], Laurence Buisseret[6,7], Vinu José[6,7], Sandra Pommey[1,2,3], Vincent Delisle[1,2,3], Sherene Loi[8,9], Heikki Joensuu[10], Pirkko-Liisa Kellokumpu-Lehtinen[11], Christos Sotiriou[6,7], Mark J. Smyth[4,5], and John Stagg[1,2,3]

Abstract

Expression of the ectonucleotidase CD73 by tumor cells, stromal cells, and immune cells is associated in cancer with immune suppression. In this study, we investigated the role of CD73 on the activity of the anti-HER2/ErbB2 monoclonal antibody (mAb) trastuzumab. In a prospective, randomized phase III clinical trial evaluating the activity of trastuzumab, high levels of CD73 gene expression were associated significantly with poor clinical outcome. In contrast, high levels of PD-1 and PD-L1 were associated with improved clinical outcome. In immunocompetent mouse models of HER2/ErbB2–driven breast cancer, CD73 expression by tumor cells and host cells significantly suppressed immune-mediated responses mediated by anti-ErbB2 mAb. Furthermore, anti-CD73 mAb therapy enhanced the activity of anti-ErbB2 mAb to treat engrafted or spontaneous tumors as well as lung metastases. Gene ontology enrichment analysis from gene-expression data revealed a positive association of CD73 expression with extracellular matrix organization, TGFβ genes, epithelial-to-mesenchymal transition (EMT) transcription factors and hypoxia-inducible-factor (HIF)-1 gene signature. Human mammary cells treated with TGFβ or undergoing EMT upregulated CD73 cell-surface expression, confirming roles for these pathways. In conclusion, our findings establish CD73 in mediating resistance to trastuzumab and provide new insights into how CD73 is regulated in breast cancer. *Cancer Res; 77(20); 5652–63. ©2017 AACR.*

Introduction

The ecto-5′-nucleotidase CD73 causes accumulation of extracellular adenosine in the tumor microenvironment (TME), thereby promoting tumor immune escape, metastasis, and resistance to immune checkpoint inhibitors (1). Extracellular adenosine mediates its immunosuppressive activity essentially by activating the high-affinity A2A and low-affinity A2B receptors. Several studies have demonstrated that targeting CD73 or A2A receptors promote antitumor immunity, have nonredundant therapeutic effects, and synergize with T-cell checkpoint inhibitors, chemotherapy, or adoptive cell therapy (2, 3). Phase I clinical trials are currently underway evaluating anti-CD73 mAbs or A2A antagonists in cancer patients, including in combination with PD-1/PD-L1 inhibitors (NCT02655822, NCT02403193, and NCT02503774).

We and others demonstrated that high levels of CD73 in the TME are generally associated with worse prognosis (4–8). In some cases, CD73 expression abrogates the good prognosis associated with tumor-infiltrating $CD8^+$ lymphocytes (TIL), consistent with its immunosuppressive function (9). In human breast cancer, we recently showed that CD73 expression negatively correlates with estrogen receptor (ER) signaling and is associated with poor prognosis and chemoresistance in the triple-negative subtype (6).

In the current study, we investigated the prognostic impact of CD73 in $HER2^+$ breast cancer in the context of trastuzumab therapy. Although anti-ErbB2 mAbs, such as trastuzumab, significantly increase survival of patients with $HER2^+$ breast cancer (10, 11), acquired and *de novo* resistance remain important challenges (12). In addition to targeting HER2 signaling, trastuzumab stimulates antitumor immunity (13–15). In support of a critical role for antitumor immunity in clinical responses to trastuzumab, high levels of TIL at diagnosis are associated with improved clinical outcomes, and patients with weak tumor immune gene signatures are less likely to benefit from trastuzumab treatment (16, 17). Yet, the value of TIL in predicting trastuzumab responses remains controversial (18).

Several immune effector pathways participate in trastuzumab activity, including natural killer (NK) cell–mediated antibody-dependent cellular cytotoxicity and adaptive $CD8^+$ T-cell responses (13). Given the importance of immune cells for trastuzumab activity, immunotherapy could synergize with anti-ErbB2 mAbs. In support of this, we previously showed that

[1]Centre de Recherche du Centre Hospitalier de l'Université de Montréal, Québec, Canada. [2]Institut du Cancer de Montréal, Montréal, Québec, Canada. [3]Faculté de Pharmacie, Université de Montréal, Québec, Canada. [4]Immunology in Cancer and Infection Laboratory, QIMR Berghofer Medical Research Institute, Herston, Queensland, Australia. [5]School of Medicine, University of Queensland, Herston, Queensland, Australia. [6]Molecular Immunology Unit, Institut Jules Bordet, Université Libre de Bruxelles, Brussels, Belgium. [7]Breast Cancer Translational Research Laboratory J.-C. Heuson, Institut Jules Bordet, Université Libre de Bruxelles, Brussels, Belgium. [8]Cancer Immunology Program, Peter MacCallum Cancer Centre, East Melbourne, Victoria, Australia. [9]Sir Peter MacCallum Department of Oncology, University of Melbourne, Parkville, Victoria, Australia. [10]Helsinki University Hospital and University of Helsinki, Helsinki, Finland. [11]Faculty of Medicine and Life Sciences, University of Tampere, Tampere, Finland.

Note: Supplementary data for this article are available at Cancer Research Online (http://cancerres.aacrjournals.org/).

Corresponding Author: John Stagg, Centre de Recherche du Centre Hospitalier de l'Université de Montréal, 900 St-Denis Street, R10.428, Montreal H2X 0A9, Québec, Canada. Phone: 514-890-8000, ext. 25170; Fax: 613-9656-1411; E-mail: john.stagg@umontreal.ca

doi: 10.1158/0008-5472.CAN-17-0707

Published OnlineFirst August 30, 2017; DOI: 10.1158/0008-5472.CAN-17-0707

anti-ErbB2 mAb synergizes with PD-1 blockade in mice (13). However, clinical data suggest that the PD-1/PD-L1 pathway is infrequently engaged in human breast cancer (19). Alternative approaches are thus likely required to induce clinically relevant antitumor responses.

We hypothesized that CD73 expression may constitute an important immune-regulatory pathway involved in trastuzumab resistance. Here, we provide evidence that CD73 expression by breast cancer cells and host cells indeed promotes resistance to trastuzumab-like therapy in immunocompetent mouse models of breast cancer. We further demonstrate that targeting CD73 significantly enhances anti-ErbB2 mAb therapy, and that high levels of CD73 in human HER2$^+$ breast cancer is associated with poor clinical benefit from trastuzumab. Our study thus supports the concept that targeting the CD73-adenosine pathway may enhance the immune-mediated activity of anti-ErbB2 mAb therapy.

Materials and Methods

Mice and cell lines

H2N100 and TUBO cells originate from BALB/c MMTV-NeuT transgenic mice (14, 20). TUBO cells were obtained in 2014 from Dr. Jason Steel (University of Cincinnati, Cincinnati, OH) and used within less than 10 freeze-thaw cycles. H2N100 cells were derived in the laboratory of Dr. Mark J. Smyth (QIMR Berghofer Medical Research, Herston, Queensland, Australia) and used within less than 10 freeze-thaw cycles. TUBO were cultured in complete DMEM 10% serum, and H2N100 were cultured in RPMI 10% serum with nonessential amino acid, Hepes, glutamax, and sodium pyruvate. Human breast cancer cell lines SKBR3 and HCC1954 were purchased from the ATCC in 2015 by the laboratory of Dr. John Stagg (University of Montreal, Québec, Canada), cultured in DMEM 10% serum and used within less than 10 freeze-thaw cycles. HMLE-TWIST-ER cells (21) were obtained in 2015 from Dr. Robert Weinberg (Whitehead Institute for Biomedical Research, Cambridge, MA), cultured in MEGM medium (Lonza), and used within less than 10 freeze-thaw cycles. No cell lines were authenticated. All cell lines were cultured at 37°C under humidified conditions and 5% CO_2, and routinely tested for *Mycoplasma* (MycoAlert Detection Kit from Lonza; cells were tested within 1 week before experimental use). Wild-type (WT) BALB/c mice were purchased from Charles Rivers Laboratories. CD73-deficient (CD73$^{-/-}$) BALB/c mice were obtained from Dr. Linda F. Thompson (Oklahoma Medical Research Foundation, Oklahoma City, OK) and maintained at the Centre de Recherche du Centre Hospitalier de l'Université de Montréal (CRCHUM; Québec, Canada). BALB/c MMTV-NeuT mice were maintained at QIMR Berghofer Medical Research Institute (Herston, Queensland, Australia). Animal studies have been conducted in accordance with an Institutional Animal Care and Use Committee.

CD73 expression

Mouse CD73 cDNA was transduced into tumor cells using a retroviral vector coexpressing GFP. Cells were sorted 5 days later by flow cytometry based on GFP expression. CD73 protein expression on transduced tumor cells was stable after *in vivo* injection (i.e., <10% variation). CD73 expression on mouse cells was assessed with eFluor 450-conjugated rat anti-mouse CD73 mAb (eBiosicence, 48-0731-82) or eFluor 450-conjugated IgG1k isotype control (eBioscience, 48-4301-82). CD73 expression on human cells was assessed with PE-conjugated mouse anti-human CD73 mAb (BD Biosciences, 550257) or PE-conjugated IgG1k isotype control (BD Biosciences, 555749). Samples were analyzed on LSRII Fortessa flow cytometer (BD Biosciences) and data analyzed with FlowJo software.

CD73 activity

H2N100-CD73 and TUBO-CD73 cells were plated in complete media in a flat-bottom 96-well plate (10^4 cells/well) 24 hours before the assay and washed twice with phosphate-free buffer (2 mmol/L $MgCl_2$, 25 mmol/L NaCl, 1 mmol/L KCl, 10 mmol/L glucose, and 10 mmol/L HEPES pH 7.2). AMP (40 μmol/L in phosphate-free buffer; Sigma) was then added, and cells were incubated for 60 minutes at 37°C. Where indicated, the CD73 inhibitor APCP (50 μmol/L; Sigma) was added. CD73 activity was quantified by measuring inorganic phosphate levels with the Malachite Green Phosphate Detection Kit (R&D Systems, #DY996) following the manufacturer's instructions.

Mouse studies

WT or CD73$^{-/-}$ mice were injected subcutaneously with H2N cells (5×10^5) and treated with 25 μg of anti-ErbB2 mAb (clone 7.16.4) on day 12, 16, and 20 and/or 200 μg of anti-CD73 (clone TY/23) on day 3, 8, 12, 16, and 20 injected intraperitoneally. TUBO cells were injected subcutaneously at 10^5 cells and treated with 100 μg of anti-ErbB2 and 200 μg of anti-CD73 following the same schedule. Where indicated, Nod-rag1-gamma c (NRG) mice were used. Where indicated, mice were depleted of NK cells by injecting anti-asialo GM1 antibody (Wako) or 50 μg anti-CD8b (clone 53-5.8; Bio X Cell) on day −1, 0, 7, and 14 posttumor cell injection following the manufacturer's instructions. BALB/c-MMTV-NeuT transgenic mice were treated at day 70 with 100 μg of anti-CD73 and/or anti-ErbB2 twice weekly for 6 weeks. Tumor multiplicity was assessed two times a week. For lung metastases studies, H2N cells (2×10^5 cells) were injected intravenously to WT mice and treated on day 8 with 250 μg of anti-CD73 and/or 10 μg of anti-ErbB2 mAbs intraperitoneally. Lungs were harvested on day 20, washed in PBS, and fixed in Bouin's solution for 24 hours before counting tumor nodules using a dissection microscope. Anti-ErbB2 mAb, anti-CD73 mAb, and control Ig (clone 2A3) were purchased from Bio X Cell.

Flow-cytometry analysis of TILs

Tumors were harvested from a TUBO subcutaneous experiment at the indicated time and exposed to a solution of collagenase type IV (and DNAse type I; Sigma). Lymphocytes were then purified using a Percoll solution of 40% to 80%. Single-cell suspensions were then stained with a panel of fluorochrome-conjugated antibodies consisting of CD4-APC (BD Biosciences, 553051), CD8a-APC-H7 (BD Biosciences, 560182), TCRb-PE (BD Biosciences, 553172), CD49b-BV421 (BD Biosciences, 563063), CD45.2-Alexa700 (eBioscience, 56-0454-82), and viability dye eF506 (eBioscience, 65-0866-14). Where indicated, cells were stained for CD11b (BD Biosciences, 561689), Gr1 (BD Biosciences, 553124), and CD73 (eBiosicence, 48-0731-82). Where indicated, cell suspensions were fixed with a Foxp3 staining buffer set (eBioscience, 00-5523-00) to be then stained for Foxp3-Alexa488 (eBioscience, 53-5773-82). Samples were analyzed on LSRII Fortessa, and data were analyzed with FlowJo software.

Published OnlineFirst August 30, 2017; DOI: 10.1158/0008-5472.CAN-17-0707

FinHER

FinHER is a phase III adjuvant clinical trial that enrolled 1,010 patients with early-stage breast cancer, 232 of whom were HER2/neu amplified and were randomly assigned to receive or not, nine weekly trastuzumab infusions in addition to chemotherapy (17). Hormone receptor status was assessed locally by IHC, and samples were considered positive if $\geq$10% cancer cells expressed receptors. HER2/neu expression was evaluated locally by IHC and confirmed centrally by *in situ* hybridization (CISH). Intratumoral and stromal TIL scores assessed on full-face hematoxylin and eosin (H&E)–stained sections were obtained for 193 HER2$^+$ patients from the analysis published by Loi and colleagues (16).

Kmplot

Kmplot is a Web-based gene-expression database, including more than 5,000 breast cancer patients associated with clinical and survival data. This database includes 1,015 untreated breast cancer patients. From those patients, 1,010 had available survival data for relapse-free survival (RFS), 543 for distant-metastasis–free survival (DMFS), 382 for overall survival (OS), and 137 for postprogression survival (PPS).

METABRIC

The breast cancer dataset disclosed by the METABRIC study is hosted by the European Bioinformatics Institute and deposited in the European Genome-Phenome Archive at http://www.ebi.ac.uk/ega/ under accession number EGAS00000000083. It contains normalized RNA microarray profiling of about 2,000 fresh-frozen breast cancer samples performed on the Illumina HT-12 v3. Hormone receptor status for the ER, HER2, and progesterone receptor (PR) were inferred based on the bimodality of their mRNA expression level using the R package genefu (version 2.6.0; ref. 22). Patients were treated either with chemotherapy, hormone-therapy, and/or radiotherapy.

Gene expression of FinHER samples

RNA was extracted from formalin-fixed, paraffin-embedded primary breast tumor tissue. All samples were reevaluated to ensure that tumor was present in the specimen. Of the 232

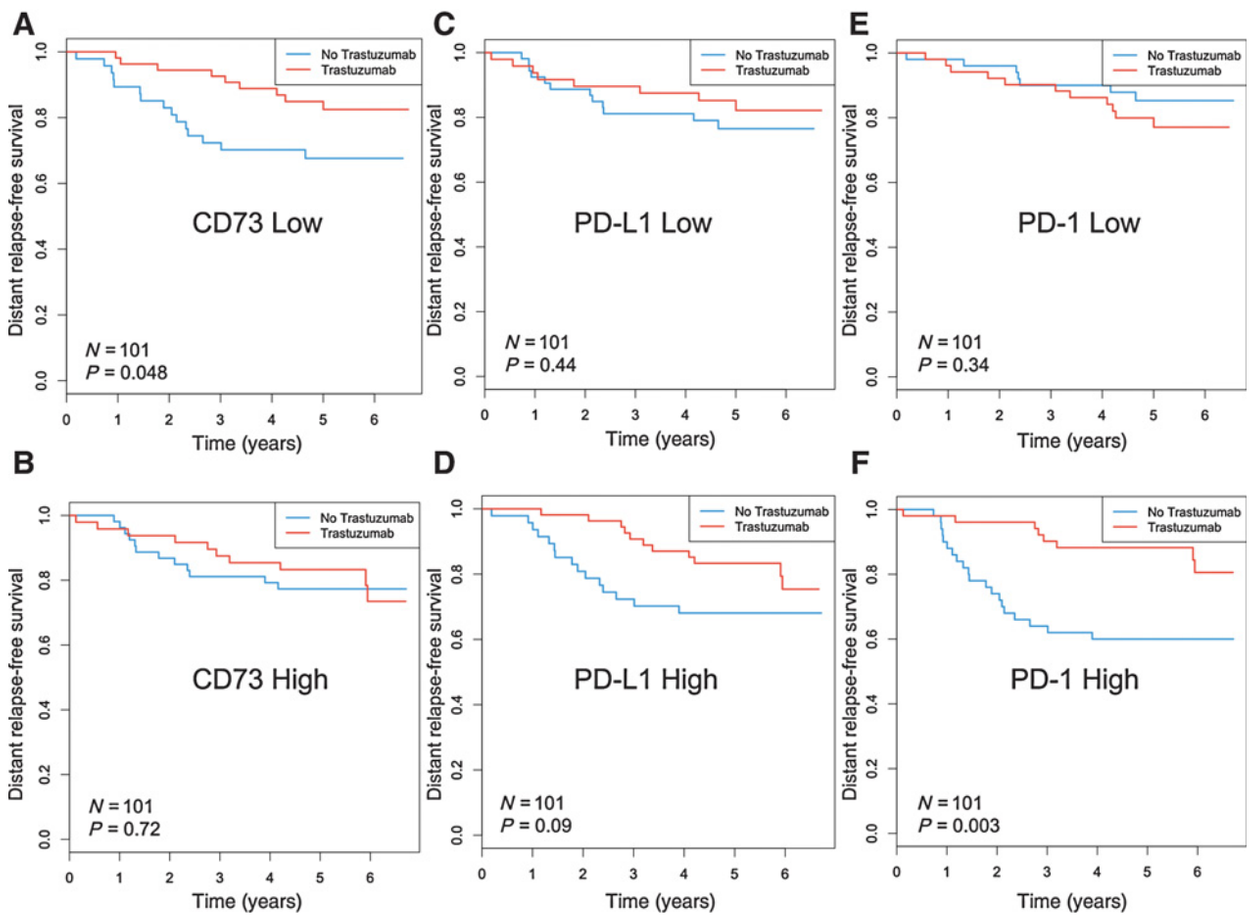

Figure 1.

High CD73 gene expression is associated with poor clinical benefit from trastuzumab in HER2$^+$ breast cancer. RFS data of 202 cases of *HER2* gene-amplified breast cancer patients randomized to receive trastuzumab or not (FinHER clinical trial) were analyzed according to) CD73 gene expression (**A** and **B**); PD-L1 gene expression (**C** and **D**); PD-1 gene expression (**E** and **F**). Significance (*P* values) of differences in survival between groups of patients defined by median gene expression was estimated by the log-rank test.

Published OnlineFirst August 30, 2017; DOI: 10.1158/0008-5472.CAN-17-0707

FinHER HER2$^+$ cases, 202 (87%) samples had sufficient good quality RNA for gene-expression analysis. Gene expression was measured using Affymetrix U219 GeneChips as per Affymetrix protocols on 96-well plates at AROS Applied Biotechnology A/S. Affymetrix expression data were normalised using the RMA approach followed by a batch effect correction [affy (v. 3.1.2) and SVA (v. 3.10.0) packages of the R (v. 3.1.2)/Bioconductor (v. 2.6) suite]. When multiple probe sets mapped to the same official gene symbol, we computed the average value of their intensity.

Correlation analyses

Gene ontology (GO) enrichment was performed using bc-GenExMiner v4.0, a publically available statistical mining tool of published annotated genomic data (23). Using bc-GenExMiner v4.0, a Robust Molecular Subtype Predictors Classification (RMSPC) was used to identify 124 patients classified in the HER2 molecular subtype, with six molecular subtype predictors. GO enrichment identified overrepresented terms present in the list of genes most positively correlated with CD73 (*NT5E*). For each term of each of the GO trees (biological process), comparison is done between the number of occurrences of this term in the "target list," that is, the number of times this term is directly linked to a gene, and the number of occurrences of this term in the "gene universe" (all of the genes that are expressed in the database) by means of the Fisher exact test. Terms with associated *P* values less than 0.01 are kept. For targeted correlation analyses, we used the breast cancer dataset disclosed by the METABRIC study. A list of top CD73 positively correlated genes was computed using cBioportal.org on 224 cases of the METABRIC study classified as HER2-enriched by PAM50. For HIF-1 signature, a signature score was calculated as a mean of the normalized expressions of its genes (i.e., P4HA1, P4HA2, PLOD1, PLOD2, LOX, LOXL2, ANGPTL4, VEGF, SLC2A1; ref. 24). The degree of association between CD73 expression and the expression of target genes (or signature) was performed using Pearson correlation.

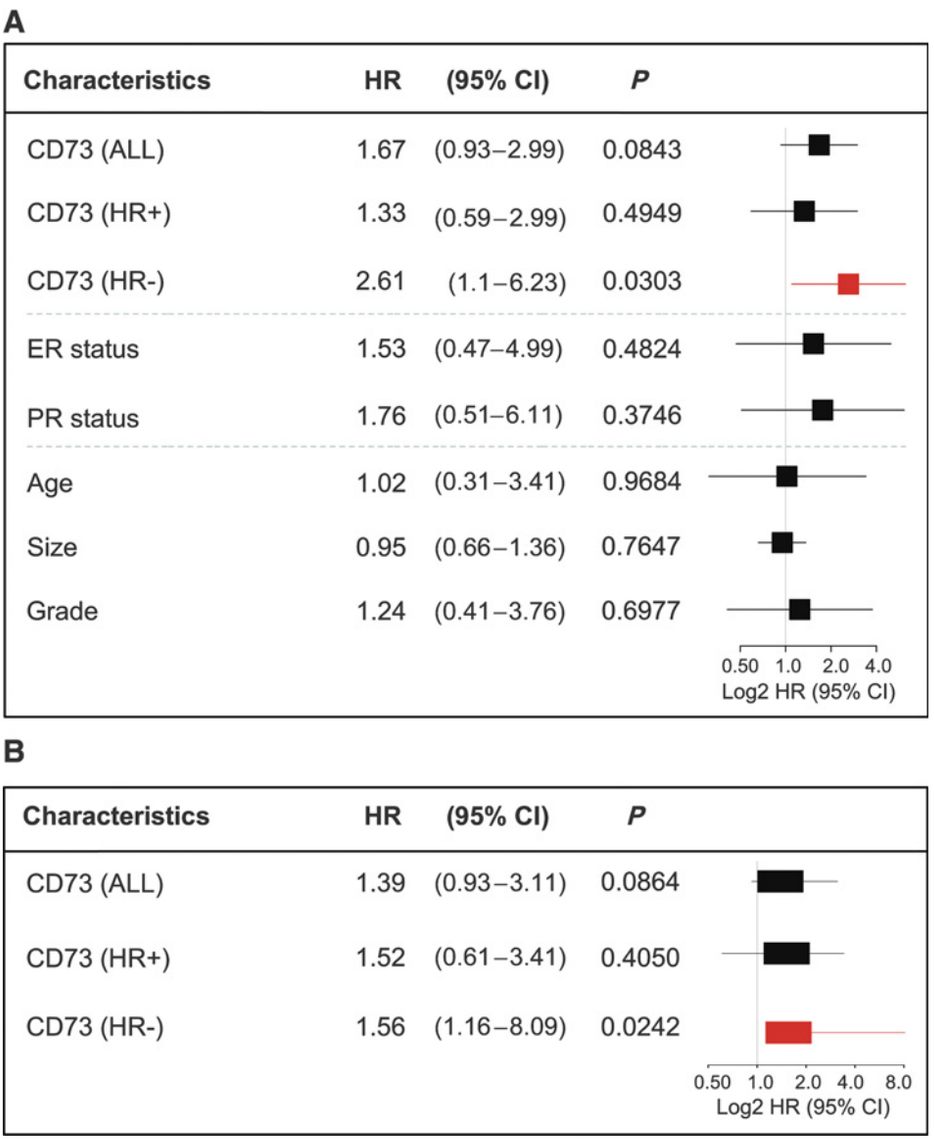

Figure 2.
CD73 interaction with trastuzumab in the FinHER clinical trial. **A,** Interaction test with trastuzumab for DRFS. Significant associations ($P < 0.05$) are shown in red. Horizontal bars represent the 95% confidence intervals (CI) of hazard ratios (HR). **B,** Interaction test for CD73, according to hormonal status (HR), with trastuzumab for DRFS, adjusted for age, nodal status, and grade. Significant associations ($P < 0.05$) after correction for multiple testing are shown in red. Horizontal bars represent the 95% CI of HRs.

Published OnlineFirst August 30, 2017; DOI: 10.1158/0008-5472.CAN-17-0707

In vitro studies

TUBO cells were treated with 10 ng/mL mouse recombinant TGFβ (R&D Systems, 7666-MB-005) and SKBR-3 cells were treated with recombinant 10 ng/mL human recombinant TGFβ (R&D Systems, 240-B-002). Cell media were changed every 2 days with fresh TGFβ. CD73 expression on TUBO and SKBR-3 cells was measured by flow cytometry. SKBR-3 cells were treated *in vitro* with 10 μg/mL of trastuzumab (obtained from CRCHUM pharmacy) and CD73 expression measured by flow cytometry. HMLE-TWIST-ER cells were induced with 20 nmol/L of 4-hydroxytamoxifen (OHT) for 12 days. CD24 (BD Biosciences, 555427) and CD44 (BD Biosciences, 559942) expression was measured by flow cytometry at different time points. For CD73 gene editing, HMLE-TWIST-ER cells were transfected with a CRISPR/Cas9 vector (px330, Addgene) expressing the 20- mer target sequences GACGCCGGCGACCAGTACCA (exon1) and GCAGCACGTTGGGTTCGGCG (exon1), provided by Michael Hoelzel (University of Bonn, Bonn, Germany). $CD73^{-}$ cells (approximately 10% of total transfected cells) were sorted by flow cytometry for further studies.

Statistical analysis

The prognostic value of gene-expression levels from selected genes and their possible interaction with trastuzumab treatment were assessed using Cox proportional hazard models. Median values of gene expression were used to divide high- and low-expression groups of patients. Distant relapse-free survival (DRFS) was compared using Kaplan–Meier analysis, and statistical significance was examined using the log-rank test. Multivariate logistic regression models (genefu R package) were also performed to assess the robustness of our result when accounting for covariates, including age (as continuous), tumor size (as continuous), nodal status (positive vs. negative), and ER status (positive vs. negative). Possible interactions with trastuzumab treatment were tested using a Wald test after adding a trastuzumab main effect and a product interaction term in the Cox model. Interaction effects were displayed using forest plots. Associations between two parameters were evaluated by a Pearson correlation. All *P* values were two-sided, and a *P* value of less than 0.05 was considered statistically significant. All statistical analyses of clinical data were performed using R v.3.2.5. ("R: The R Project for Statistical Computing," 2016; https://www.r-project.org).

Results

CD73 is associated with trastuzumab resistance

We first assessed the prognostic value of CD73 in untreated breast cancer patients. CD73 expression was found to be significantly associated with worse disease-free survival in all untreated breast cancer as well as in untreated $HER2^{+}$ breast cancer (Supplementary Fig. S1). Higher CD73 expression was also associated with a worse disease-specific survival in the METABRIC cohort, but this association was not significant in the $HER2^{+}$ subtype (Supplementary Fig. S2). We then assessed whether CD73 gene expression in the $HER2^{+}$ subtype was specifically associated with therapeutic benefit from trastuzumab. Using gene expression profiles of 202 cases of the FinHER

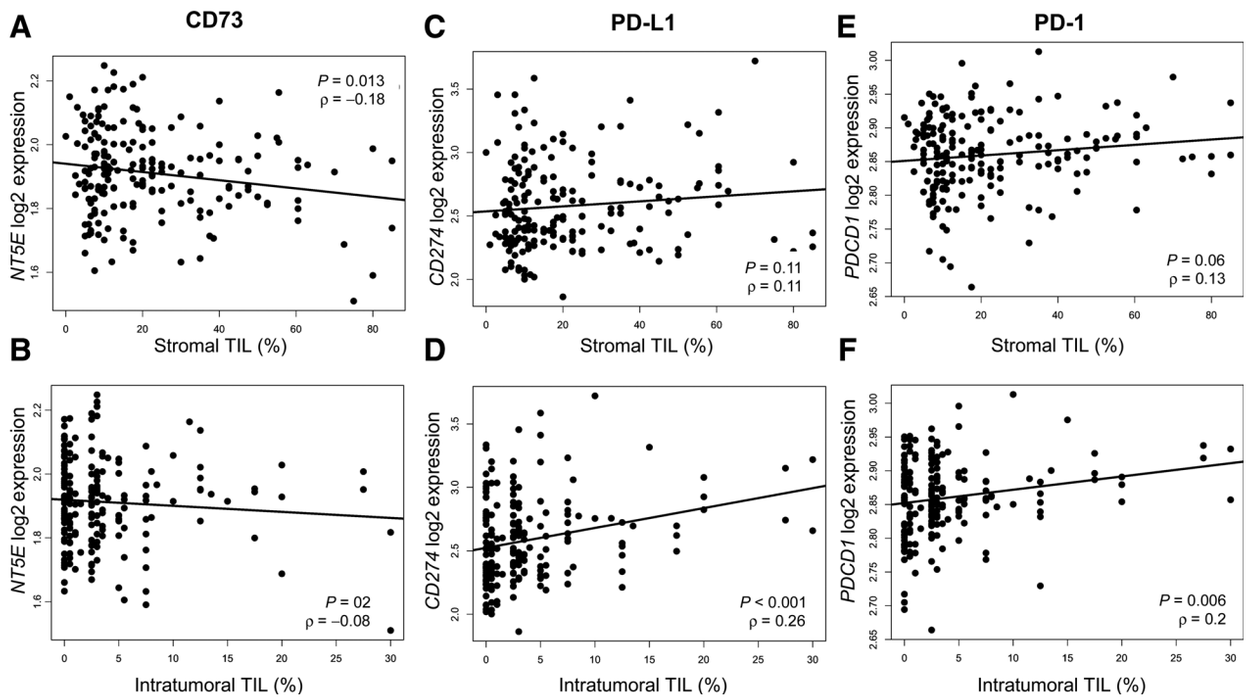

Figure 3.

PD-1 and PD-L1, but not CD73, correlate with tumor-immune infiltrates in $HER2^{+}$ breast cancer. Stromal and intratumoral TIL assessed on full-face H&E sections of *HER2* gene-amplified breast tumors from FinHER were correlated to CD73 gene expression (**A** and **B**); PD-L1 gene expression (**C** and **D**); PD-1 gene expression (**E** and **F**). Correlation coefficients (Spearman rho) with *P* values are shown.

Published OnlineFirst August 30, 2017; DOI: 10.1158/0008-5472.CAN-17-0707

clinical trial confirmed to have *HER2* gene amplification and randomly assigned to receive or not short-course adjuvant trastuzumab (17), we compared DRFS according to CD73 expression levels. As shown in Fig. 1A and B, patients with low levels of CD73 (below median) significantly benefited from trastuzumab (Fig. 1A; $P = 0.048$ by log rank), whereas patients with high levels of CD73 (above median) showed no significant benefit (Fig. 1B; $P = 0.72$ by log rank). For comparison, we also assessed the prognostic value of PD-L1 and PD-1 gene expression. In contrast with CD73, high levels of PD-L1 (Fig. 1C and D) or PD-1 (Fig. 1E and F) were associated with improved clinical benefit from trastuzumab ($P = 0.09$ and $P = 0.003$ by log rank, respectively). Multivariate analysis supported these results (Supplementary Fig. S3). To confirm that CD73 was associated with trastuzumab responses, we performed interaction tests for DRFS. As shown in Fig. 2A, there was a significant interaction between CD73 expression and trastuzumab in hormonal receptor (HR)–negative patients ($P = 0.0303$), but not in HR$^+$ patients ($P = 0.4949$). This interaction was still significant when adjusted for age, nodal status, and grade ($P = 0.0242$; Fig. 2B). We next evaluated whether CD73 expression correlated with TILs, as previously quantified on H&E-stained sections (16). We observed a weak negative correlation between CD73 and stromal TIL (Fig. 3A) and no correlation between CD73 and intratumoral TIL (Fig. 3B). In contrast, both PD-L1 and PD-1 gene expression positively correlated with intratumoral TIL (Fig. 3C–F).

CD73 on tumor cells confers resistance to anti-ErbB2 mAb

Using immunocompetent mouse models of HER2$^+$ breast cancer, we further investigated the impact of CD73 expression on anti-ErbB2 mAb therapy. H2N100 and TUBO breast tumor cells, derived from NeuT-transgenic mice and endogenously negative for CD73, were gene modified to overexpress CD73 or control vector (Supplementary Fig. S4), injected subcutaneously to syngeneic mice, and treated with anti-ErbB2 mAb (clone 7.16.4). As shown in Fig. 4A and B (and Supplementary Fig. S5), CD73 overexpression on H2N100 tumors significantly suppressed the activity of anti-ErbB2 mAb. Accordingly, while anti-ErbB2 mAb induced complete responses (CR) in 100% (20/20) of mice with CD73$^-$ H2N100 tumors, only 25% (5/20) of mice bearing CD73$^+$ tumors achieved CR (Supplementary Fig. S5; $P < 0.0001$ by log rank). CD73 overexpression on TUBO cells was also associated with reduced anti-ErbB2 mAb

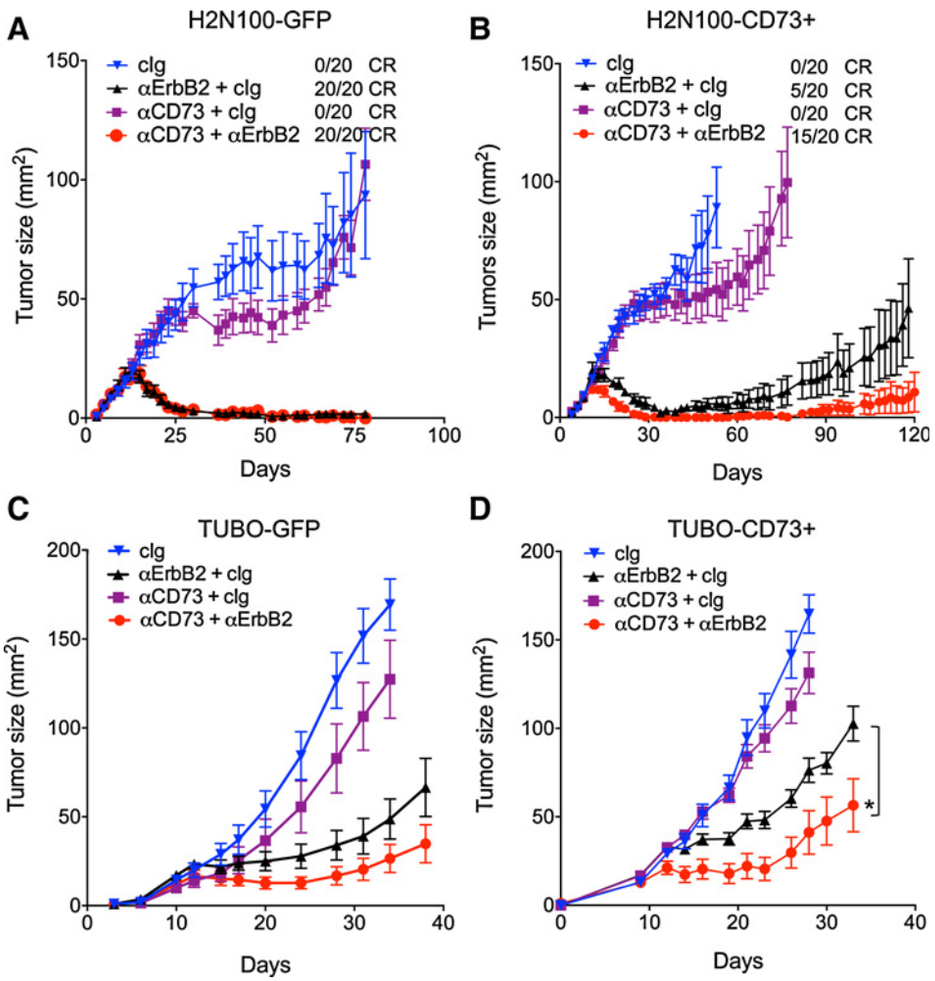

Figure 4.
CD73 expression by breast tumor cells inhibits anti-ErbB2 mAb activity. **A** and **B,** BALB/c mice were injected subcutaneously with H2N100-GFP or H2N100-CD73$^+$ breast tumor cells and treated with anti-ErbB2 mAb (25 μg intraperitoneally of clone 7.16.4) on day 12, 16, and 20, and/or anti-CD73 mAb (200 μg intraperitoneally of clone TY/23) on day 3, 8, 12, 16, and 20. Means ± SE ($n = 10$/group) of one representative experiment are shown. Number of mice achieving complete response (CR) from two independent experiments is shown. **C** and **D**, BALB/c mice were injected subcutaneously with TUBO-GFP or TUBO-CD73$^+$ breast tumor cells and treated with anti-ErbB2 mAb (100 μg intraperitoneally of clone 7.16.4) on day 12, 16, and 20, and/or anti-CD73 mAb (200 μg intraperitoneally of clone TY/23) on day 3, 8, 12, 16, and 20. Means ± SE ($n = 10$/group) of one representative experiment are shown (*, $P < 0.05$ by Mann–Whitney test).

Published OnlineFirst August 30, 2017; DOI: 10.1158/0008-5472.CAN-17-0707

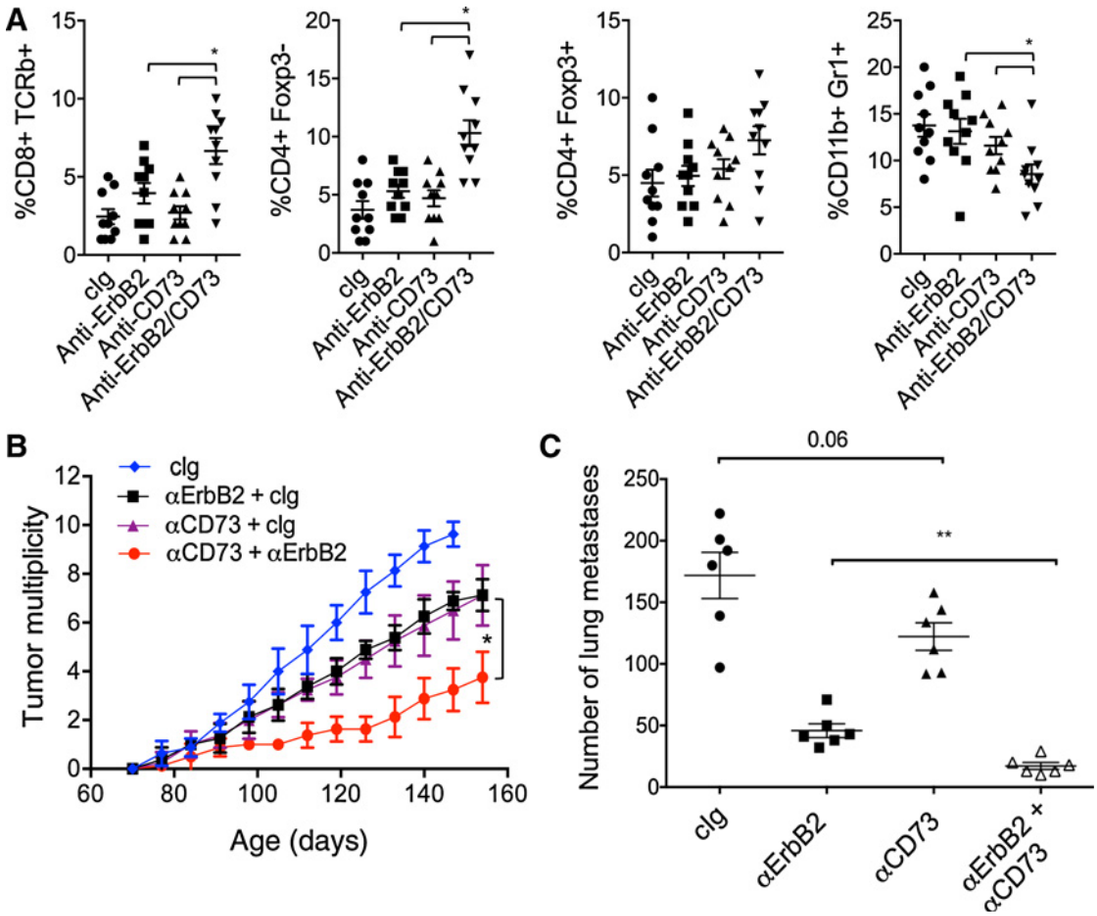

Figure 5.

Anti-CD73 mAb enhances anti-ErbB2 mAb therapy. **A,** BALB/c mice were injected subcutaneously with TUBO-CD73$^+$ cells and treated with anti-ErbB2 mAb (100 μg intraperitoneally of clone 7.16.4) on day 12 and 16 and/or anti-CD73 mAb (200 μg intraperitoneally of clone TY/23) on day 3, 8, 12, and 16. Tumors were harvested at day 20 for flow cytometry analysis. Frequencies of tumor-infiltrating CD8$^+$ T cells, CD4$^+$ Foxp3$^-$ T cells, CD4$^+$ Foxp3$^+$ T cells, and CD11b$^+$ Gr1$^+$ cells in CD45.2$^+$ cells are shown. Means ± SE are shown (*, $P < 0.05$ by Mann-Whitney test). **B,** BALB/c-MMTV-NeuT transgenic mice were treated from day 70 with anti-CD73 mAb (TY/23) and/or anti-ErbB2 mAb (7.16.4) for 6 weeks (100 μg each, intraperitoneally). Mean tumor multiplicity ± SE are shown ($n = 10$/group; *, $P < 0.05$ by Mann–Whitney test at endpoint). **C,** H2N100 tumor cells (2×10^5 cells) were injected intravenously into WT BALB/c mice and treated on day 8 with 250 μg of anti-CD73 mAb and/or 10 μg of anti-ErbB2 (intraperitoneally). Lungs were harvested on day 20, fixed, and lung tumor nodules counted using a dissection microscope. Individual nodule counts with means ± SE are shown (**, $P < 0.01$ by Mann–Whitney test).

activity (Fig. 4C and D; Supplementary Fig. S5; $P < 0.0001$ by log rank), although no CR was achieved in this model.

Targeting CD73 enhances the activity of anti-ErbB2 mAb

We next assessed whether targeting CD73 could enhance trastuzumab-like therapy. As shown in Fig. 4 and Supplementary Fig. S5, combining anti-CD73 mAb with anti-ErbB2 mAb was significantly more effective than either single agent. In H2N100-CD73$^+$ tumors, the combined therapy induced CR in 75% of mice (15/20) compared with 25% CR (5/20) for anti-ErbB2 mAb and 0% CR (0/20) for anti-CD73 mAb. Anti-CD73 mAb also significantly enhanced the activity of anti-ErbB2 mAb against TUBO-CD73$^+$ tumors, although no CR was achieved. In support of an immune-dependent mechanism, the benefit of combining anti-ErbB2 mAb with anti-CD73 mAb was lost in immunodeficient NOD-Rag1-γc mice (Supplementary Fig. S6). Also, consistent with increased anti-tumor immunity, combined treatment significantly enhanced tumor-infiltrating CD8$^+$ T cells and CD4$^+$ Foxp3$^-$ T cells (Fig. 5A). Interestingly, combining anti-ErbB2 with anti-CD73 mAb also significantly reduced tumor-infiltrating CD11b$^+$ Gr1$^+$ myeloid cells, although no significant effect was observed on CD4$^+$ Foxp3$^+$ regulatory T cells (Tregs; Fig. 5A).

We next evaluated the therapeutic activity of the combination on autochthonous ErbB2-driven tumors spontaneously arising in BALB/c-NeuT transgenic mice. Cohorts of transgenic female mice were treated from day 70 twice a week with intraperitoneal injections of anti-CD73 mAb, anti-ErbB2 mAb, or anti-CD73 + anti-ErbB2 mAbs, and tumor multiplicity (i.e., tumor occurrence in the 10 mammary glands) monitored over time. As shown in Fig. 5B, the combination therapy was significantly more effective than either monotherapy. We also evaluated the anti-

Published OnlineFirst August 30, 2017; DOI: 10.1158/0008-5472.CAN-17-0707

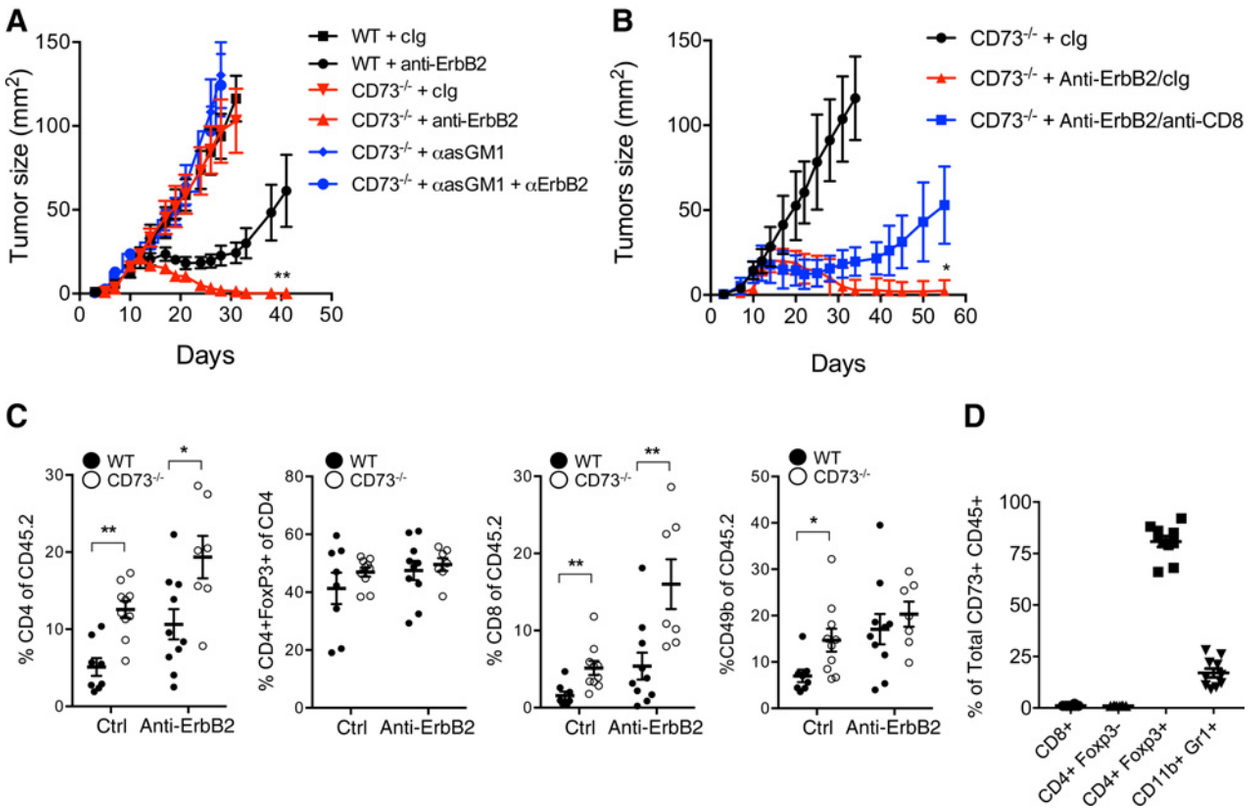

Figure 6.

Host CD73 inhibits anti-ErbB2 mAb activity. **A,** WT and CD73$^{-/-}$ BALB/c mice were injected subcutaneously with TUBO cells and treated with anti-ErbB2 mAb (100 μg intraperitoneally of clone 7.16.4) on day 12, 16, and 20. Some mice were further depleted of NK cells (anti-asialo GM1 antibody), or depleted of CD8$^+$ T cells, on day −1, 0, 7, and 14 (**B**). Means ± standard errors ($n = 10$/group) are shown (**, $P < 0.01$ by Mann-Whitney test). **C,** Same as **A**, except that TUBO tumors were harvested at day 19 for flow cytometry analysis. Frequencies of CD4$^+$ T cells, Foxp3$^+$ Tregs, CD8$^+$ T cells, and CD49b$^+$ NK cells are shown. Means ± SE are shown (*, $P < 0.05$; **, $P < 0.01$ by Mann–Whitney test). **D,** WT BALB/c mice were injected with TUBO cells and treated as in **A**, and frequencies of indicated cells within CD73$^+$ CD45$^+$ tumor-infiltrating cells are shown. Means ± SE are shown.

metastatic activity of the combination therapy and observed that anti-CD73 mAb significantly enhanced the activity of anti-ErbB2 mAb against experimental lung metastases (Fig. 5C). Taken together, our data demonstrated that CD73 promotes resistance to anti-ErbB2 mAb and that targeting CD73 can overcome this resistance.

Host CD73 confers resistance to anti-ErbB2 mAb

Because CD73 is found expressed on both tumor cells and non-transformed cells, we investigated the role of host-derived CD73 using CD73-deficient mice. As shown in Fig. 6A, anti-ErbB2 mAb therapy was significantly more effective in CD73-deficient mice, inducing CR in 100% of mice (10/10) compared with 0% in WT mice (0/10). Notably, this enhanced activity in CD73$^{-/-}$ mice was lost upon NK cell depletion (Fig. 6A). Long-term control in CD73$^{-/-}$ mice was also lost upon CD8$^+$ T-cell depletion (Fig. 6B). Flow cytometry analyses revealed a significant increase in NK cells, CD4$^+$ T_{conv} cells, and CD8$^+$ T cells in response to anti-ErbB2 mAb in CD73$^{-/-}$ mice compared with WT (Fig. 6C). When tumor-infiltrating host cells expressing CD73 were analyzed, we found that the vast majority were CD4$^+$Foxp3$^+$ Tregs, followed by CD11b$^+$ Gr1$^+$ myeloid cells (Fig. 6D).

CD73 expression is associated with HIF-1, TGFβ, and EMT

We next investigated underlying pathways associated with CD73 expression in HER2$^+$ breast cancer. Since CD73 is a transcriptional target of HIF-1α (25), we first assessed the correlation between CD73 and a HIF-1 gene signature derived in human breast cancer (24). We observed a significant, albeit weak, positive correlation between CD73 expression and HIF-1 responses (Fig. 7A). We next performed GO enrichment analysis and found a significant association between CD73 and extracellular matrix organization (Table 1). Correlative analyses further revealed that 8 of the 10 most positively correlated genes in HER2-enriched breast cancer were linked to TGFβ (Table 1). We thus investigated whether TGFβ regulated CD73 expression in HER2$^+$ breast tumor cells. As shown in Fig. 7B and C, treatment with recombinant TGFβ significantly induced CD73 expression on both mouse and human HER2$^+$ breast tumor cells. Interestingly, CD73 upregulation in SKBR-3 in response to TGFβ was maximal approximately 20 days after treatment initiation (Fig. 7B), suggesting that cellular reprogramming, in contrast to direct signaling, might be involved. CD73 upregulation in mouse TUBO cells reached a maximum after 48 hours (Fig. 7B). TGFβ is a potent inducer of epithelial-to-mesenchymal transition (EMT; ref. 26). We hypothesized that EMT regulated CD73 expression in mammary cells. Consistent

Published OnlineFirst August 30, 2017; DOI: 10.1158/0008-5472.CAN-17-0707

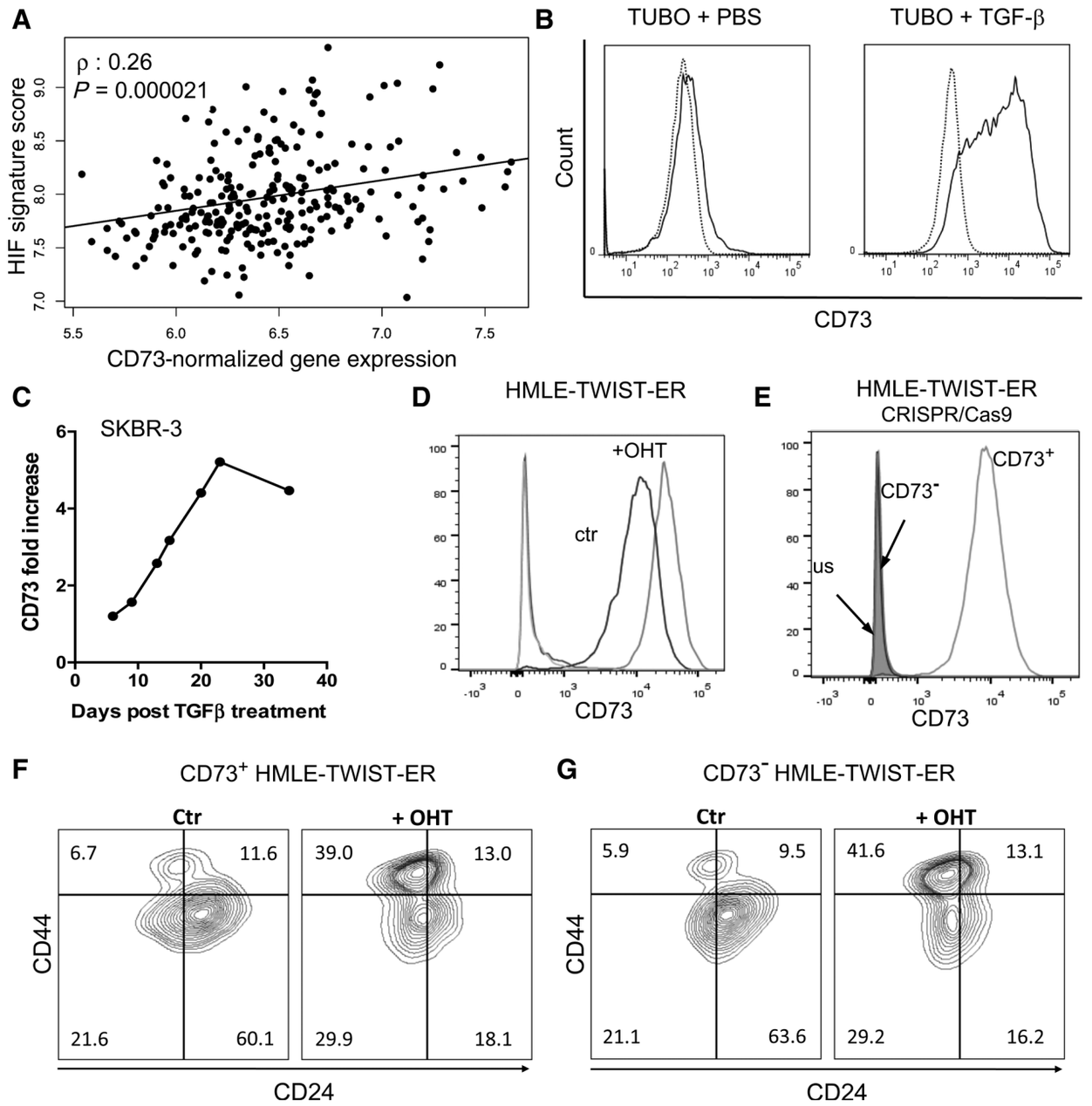

Figure 7.

Association between CD73, HIF-1, TGFβ, and EMT. **A,** The degree of association between CD73 gene expression and the expression of an HIF-1 gene signature was performed in HER2$^+$ cases in METABRIC. Pearson coefficient and *P* value are shown. Mouse TUBO (**B**) and human SKBR-3 (**C**) breast tumor cells were treated with recombinant TGFβ (10 ng/mL), and CD73 expression was measured by flow cytometry after 48 hours (**B**) or at indicated time points (**C**). Fold increase of mean fluorescence intensity over PBS-treated cells is shown. **D,** HMLE-TWIST-ER cells were treated with 20 nmol/L 4-hydroxytamoxifen (OHT) for 12 days, and CD73 expression was measured by flow cytometry. **E,** HMLE-TWIST-ER were transfected with two CRISPR/Cas9 vectors containing sgRNA against CD73 and sorted into CD73$^+$ and CD73$^-$ cells. **F** and **G**, CD73$^+$ and CD73$^-$ HMLE cells were treated with 20 nmol/L 4-hydroxytamoxifen (OHT) for 12 days, and CD24/CD44 expression was measured by flow cytometry.

with this, CD73 was significantly and positively correlated with several EMT transcription factors in HER2$^+$ breast tumors, with a notable exception for *SNAI1* (Supplementary Fig. S7). To assess whether EMT promoted CD73 expression, we used human mammary epithelial cells (HMLE) expressing an inducible TWIST1 (i.e., HMLE-TWIST-ER cells). As shown in Fig. 7D, activation of EMT indeed significantly upregulated CD73 cell-surface expression on HMLE cells. To determine whether CD73 was required for EMT, we performed CRISPR-mediated editing of CD73 in HMLE cells (Fig. 7E). As shown in Fig. 7F and G, lack of CD73 had no impact

Published OnlineFirst August 30, 2017; DOI: 10.1158/0008-5472.CAN-17-0707

Table 1. CD73 Gene Ontology enrichment and top genes correlated to CD73

GO term and associated genes	*P*	% target list	% universe
Extracellular matrix organization:			
COL27A1, CTSK, LOX, DCN, ITGA11, TIMP2, MFAP2, ECM2, MMP13, THBS1, PLOD2, POSTN	7.37e−09	17.65	1.97
Gene	**Spearman rho**	**KEGG pathway**	**Other pathway**
CLIC4	0.67	Adherens junction/Fc-gamma/Cell cycle/Tight junction	TGFβ
CTHRC1	0.66	n/a	TGFβ, EMT
GAS1	0.64	Hedgehog/NOD-like/Apoptosis/Ubiquitin	WNT
DSE	0.64	n/a	(TGFβ)
THBS1	0.64	ECM/Adhesion/Actin/TGF/Cytokine	TGFβ
ACSL4	0.63	PPAR/Adipocytokine	Ferroptosis
FNDC1	0.63	n/a	TGFβ
COL10A1	0.63	n/a	TGFβ
CD55	0.63	T cell/NK cell/Adherens junction	TGFβ
LUM	0.63	ECM/GnRH/Spliceosome	TGFβ

on the expression of EMT surrogate markers ($CD44^{high}CD24^{low}$). Overall, our study highlights the importance of CD73 in trastuzumab resistance and suggests that targeting the CD73-adenosine pathway, or upstream regulators such as TGFβ or EMT, may enhance immune-mediated responses induced by anti-ErbB2 mAb therapy.

Discussion

Immune infiltrates in HER2/ErbB2$^+$ breast tumors are associated with improved survival and contribute to the therapeutic activity of trastuzumab (16). With the general objective to identify novel actionable immunosuppressive pathways, we here report the role of CD73 on the activity of anti-ErbB2 antibody therapy. Our study demonstrated that: (i) high levels CD73, but not PD-1 or PD-L1, are associated with increased resistance to trastuzumab; (ii) CD73 expression by breast tumor cells and host cells suppresses immune-mediated antitumor responses induced by anti-ErbB2 mAb therapy in mice; (iii) targeted blockade of CD73 enhances anti-ErbB2 mAb therapy in mice; and (iv) CD73 expression in human mammary cells is induced by TGFβ and EMT.

Several environmental factors have been shown to promote activation of adenosine signaling in the TME, including tissue hypoxia, HIF-1α, and inflammatory cytokines (27). CD73 promoter methylation and ER signaling have also been shown to regulate CD73 expression in melanoma and breast cancer (28–30). Consistent with a role for tissue hypoxia in regulating extracellular adenosine levels, we observed a positive correlation between CD73 expression and HIF-1 responses in HER2$^+$ breast tumors. We further demonstrated that TGFβ and EMT are important inducers of CD73 expression in human mammary cells. Interestingly, EMT has been shown to be associated with trastuzumab resistance (31, 32), and TGFβ was recently identified as a major pathway disabling antitumor immunity in human breast cancer (33). We propose that CD73 and adenosine signaling may contribute to EMT-mediated trastuzumab resistance and TGFβ–mediated tumor immune escape.

Using GO enrichment analysis, we found an association between CD73 expression and extracellular matrix organization. In particular, CD73 positively correlated with several genes involved in collagen remodeling and previously associated with increased tumor cell metastasis, including lysyl oxidase (*LOX*), lysyl hydroxylase (*PLOD2*), cathepsin K (*CTSK*), collagen-binding integrin (ITGA11), matrix metallopeptidase-13 (*MMP13*), thrombospondin-1 (*THBS1*), and periostin (*POSTN*; refs. 34–39). Because CD73 has been shown to promote fibrosis (40), it would be of interest to evaluate whether adenosine signaling regulates any of these genes.

Our current study provides an important proof of concept that targeting CD73 significantly enhances the therapeutic activity of anti-ErbB2 mAb in immunocompetent hosts. We clearly demonstrated that tumor-derived CD73, as well as host-derived CD73, suppressed antitumor immune responses generated by anti-ErbB2 mAb. Notably, host CD73 was found to significantly suppress NK cell–mediated as well as $CD8^+$ T-cell–mediated antitumor responses. NK cells have been shown to be critical for trastuzumab activity (41), and our previous work demonstrated that interferon responses and $CD8^+$ T-cell activation generate adaptive antitumor immunity following anti-ErbB2 mAb therapy (13). We now provide evidence that host CD73 contributes to suppress both innate and adaptive antitumor immunity stimulated by anti-ErbB2 mAb treatment. Interestingly, we observed that targeting CD73 significantly reduced the level of tumor-infiltrating $CD11b^+$ $Gr1^+$ myeloid cells when combined with anti-ErbB2 mAb. Because $CD4^+$ $Foxp3^+$ Tregs can promote immunosuppressive $CD11b^+$ $Gr1^+$ cells in response to ErbB2-driven breast cancer (41), and considering that $CD4^+$ $Foxp3^+$ Tregs are a major source of host CD73, Tregs may favor the recruitment of $CD11b^+Gr1^+$ myeloid cells in the TME.

Although our study suggests that targeting the CD73-adenosine pathway can potentiate the antitumor activity of trastuzumab, further studies investigating the impact of targeting the A2A adenosine receptor would be valuable. We argue that CD73- and/or A2A-targeting therapy would be most beneficial against HER2$^+$ breast tumors that express high levels of CD73, such as mesenchymal tumors. Nevertheless, caution should be employed in restricting adenosine-targeting therapies to CD73-expressing tumors. Indeed, CD73 expression by tumor cells is not always a prerequisite to activity, as can be observed in the CT26 colon adenocarcinoma model (42).

Several anti-CD73 mAbs and antagonists to the A2A adenosine receptor are now entering clinical trials. A recent study suggested that dual targeting of CD73 and A2A receptor could generate synergistic therapeutic responses (43). Notably, it was observed that tumor CD73 expression was significantly upregulated when transplanted to A2A-deficient hosts. Although anti-CD73 mAbs can decrease adenosine levels and block adenosine's suppressive effects on immune effectors, Fc receptor engagement may also play a role in therapeutic activity. In support of this, it was shown

Published OnlineFirst August 30, 2017; DOI: 10.1158/0008-5472.CAN-17-0707

in human mixed leukocyte reactions that Fc receptor binding significantly increased production of proinflammatory cytokines upon anti-CD73 mAb (43). Consideration of the Fc domain and its interaction with immune cells may thus be important in the development of optimal anti-CD73 mAbs.

In conclusion, our current study provided clinical and experimental evidence that CD73 expression is associated with resistance to trastuzumab therapy. Given the importance of antitumor immune responses in HER2$^+$ breast cancer and the paucity of clinical responses to PD-1/PD-L1 inhibitors in this subtype, our study provides a rationale to further investigate the impact of combining adenosine-targeting agents with anti-ErbB2 mAbs for patients refractory to standard-of-care treatments.

Disclosure of Potential Conflicts of Interest

S. Loi reports receiving a commercial research grant and is a consultant/advisory board member Roche Genentech. P.-L. Kellokumpu-Lehtinen has received speakers bureau honoraria from Bureau BMS and Roche. M.J. Smyth reports receiving a commercial research grant from Bristol-Myers Squibb, Corvus, Pharmaceuticals, Aduro Biotech, Tizona Therapeutics, is a consultant/advisory board member for Arcus Biosciences, Kymab, F-star, and has provided expert testimony for Corvus Pharmaceuticals. J. Stagg reports receiving a commercial research grant from Surface Oncology and is a consultant/advisory board member for Surface Oncology, Novartis, Merck. No potential conflicts of interest were disclosed by the other authors.

Authors' Contributions

Conception and design: M. Turcotte, S. Pommey, P.-L. Kellokumpu-Lehtinen, J. Stagg

Development of methodology: M. Turcotte, S. Pommey, S. Loi, J. Stagg

Acquisition of data (provided animals, acquired and managed patients, provided facilities, etc.): M. Turcotte, D. Allard, D. Mittal, V. Delisle, S. Loi, H. Joensuu, P.-L. Kellokumpu-Lehtinen, C. Sotiriou, M.J. Smyth

Analysis and interpretation of data (e.g., statistical analysis, biostatistics, computational analysis): M. Turcotte, D. Allard, D. Mittal, Y. Bareche, L. Buisseret, V. José, V. Delisle, S. Loi

Writing, review, and/or revision of the manuscript: M. Turcotte, D. Allard, Y. Bareche, L. Buisseret, S. Loi, H. Joensuu, P.-L. Kellokumpu-Lehtinen, C. Sotiriou, M.J. Smyth, J. Stagg

Study supervision: J. Stagg

Acknowledgments

The authors thank Dominique Gauchat of the CRCHUM Cytometry core facility for performing cell sorting.

Grant Support

J. Stagg received a Project Grant from the Canadian Institutes for Health Research (CIHR). J. Stagg received a salary award from the CIHR and support from the Jean-Guy Sabourin Research Chair in Pharmacology. M. Turcotte received a doctoral scholarship from the Fonds de Recherche du Québec—Santé (FRQS). M.J. Smyth was supported by a National Health and Medical Research Council of Australia (NH & MRC) Senior Principal Research Fellowship (1078671) and Project Grant (1120887). J. Stagg and M.J. Smyth were supported by the Susan G. Komen foundation (IIR12221504). C. Sotiriou received a research grant from the Breast Cancer Research Foundation (BCRF) and from the Fonds de la Recherche Scientifique (FNRS). L. Buisseret is fellow of the FNRS.

The costs of publication of this article were defrayed in part by the payment of page charges. This article must therefore be hereby marked *advertisement* in accordance with 18 U.S.C. Section 1734 solely to indicate this fact.

Received March 15, 2017; revised July 8, 2017; accepted August 18, 2017; published OnlineFirst August 30, 2017.

References

1. Allard D, Turcotte M, Stagg J. Targeting A2 adenosine receptors in cancer. Immunol Cell Biol 2017;95:333–339.
2. Allard B, Pommey S, Smyth MJ, Stagg J. Targeting CD73 enhances the antitumor activity of anti–PD-1 and anti–CTLA-4 mAbs. Clin Cancer Res 2013;19:5626–35.
3. Beavis PA, Henderson MA, Giuffrida L, Mills JK, Sek K, Cross RS, et al. Targeting the adenosine 2A receptor enhances chimeric antigen receptor T cell efficacy. J Clin Invest 2017;127:929–41.
4. Gaudreau PO, Allard B, Turcotte M, Stagg J. CD73-adenosine reduces immune responses and survival in ovarian cancer patients. Oncoimmunology 2016;5:e1127496.
5. Leclerc BG, Charlebois R, Chouinard G, Allard B, Pommey S, Saad F, et al. CD73 expression is an independent prognostic factor in prostate cancer. Clin Cancer Res 2016;22:158–66.
6. Loi S, Pommey S, Haibe-Kains B, Beavis PA, Darcy PK, Smyth MJ, et al. CD73 promotes anthracycline resistance and poor prognosis in triple negative breast cancer. Proc Natl Acad Sci U S A 2013;110:11091–6.
7. Inoue Y, Yoshimura K, Kurabe N, Kahyo T, Kawase A, Tanahashi M, et al. Prognostic impact of CD73 and A2A adenosine receptor expression in non-small-cell lung cancer. Oncotarget 2017;8:8738–51.
8. Limagne E, Euvrard R, Thibaudin M, Rebe C, Derangere V, Chevriaux A, et al. Accumulation of MDSC and Th17 cells in patients with metastatic colorectal cancer predicts the efficacy of a FOLFOX-Bevacizumab drug treatment regimen. Cancer Res 2016;76:5241–52.
9. Turcotte M, Spring K, Pommey S, Chouinard G, Cousineau I, George J, et al. CD73 is associated with poor prognosis in high-grade serous ovarian cancer. Cancer Res 2015;75:4494–503.
10. Cobleigh MA, Vogel CL, Tripathy D, Robert NJ, Scholl S, Fehrenbacher L, et al. Multinational study of the efficacy and safety of humanized anti-HER2 monoclonal antibody in women who have HER2-overexpressing metastatic breast cancer that has progressed after chemotherapy for metastatic disease. J Clin Oncol 1999;17:2639–48.
11. Piccart-Gebhart MJ, Procter M, Leyland-Jones B, Goldhirsch A, Untch M, Smith I, et al. Trastuzumab after adjuvant chemotherapy in HER2-positive breast cancer. N Engl J Med 2005;353:1659–72.
12. Rexer BN, Arteaga CL. Intrinsic and acquired resistance to HER2-targeted therapies in HER2 gene-amplified breast cancer: mechanisms and clinical implications. Crit Rev Oncog 2012;17:1–16.
13. Stagg J, Loi S, Divisekera U, Ngiow SF, Duret H, Yagita H, et al. Anti-ErbB-2 mAb therapy requires type I and II interferons and synergizes with anti-PD-1 or anti-CD137 mAb therapy. Proc Natl Acad Sci U S A 2011;108:7142–7.
14. Charlebois R, Allard B, Allard D, Buisseret L, Turcotte M, Pommey S, et al. PolyI:C and CpG synergize with anti-ErbB2 mAb for treatment of breast tumors resistant to immune checkpoint inhibitors. Cancer Res 2017;77:312–9.
15. Pusztai L, Karn T, Safonov A, Abu-Khalaf MM, Bianchini G. New strategies in breast cancer: immunotherapy. Clin Cancer Res 2016;22:2105–10.
16. Loi S, Michiels S, Salgado R, Sirtaine N, Jose V, Fumagalli D, et al. Tumor infiltrating lymphocytes are prognostic in triple negative breast cancer and predictive for trastuzumab benefit in early breast cancer: results from the FinHER trial. Ann Oncol 2014;25:1544–50.
17. Joensuu H, Kellokumpu-Lehtinen PL, Bono P, Alanko T, Kataja V, Asola R, et al. Adjuvant docetaxel or vinorelbine with or without trastuzumab for breast cancer. N Engl J Med 2006;354:809–20.
18. Perez EA, Ballman KV, Tenner KS2, Thompson EA, Badve SS, Bailey H, Baehner FL. Association of stromal tumor-infiltrating lymphocytes with recurrence-free survival in the N9831 adjuvant trial in patients with early-stage HER2-positive breast cancer. JAMA Oncol 2016;2:56–64.
19. Savas P, Salgado R, Denkert C, Sotiriou C, Darcy PK, Smyth MJ, et al. Clinical relevance of host immunity in breast cancer: from TILs to the clinic. Nat Rev Clin Oncol 2016;13:228–41.
20. Rovero S, Amici A, Di Carlo E, Bei R, Nanni P, Quaglino E, et al. DNA vaccination against rat her-2/Neu p185 more effectively inhibits carcinogenesis than transplantable carcinomas in transgenic BALB/c mice. J Immunol 2000;165:5133–42.

21. Casas E, Kim J, Bendesky A, Ohno-Machado L, Wolfe CJ, Yang J. Snail2 is an essential mediator of Twist1-induced epithelial mesenchymal transition and metastasis. Cancer Res 2011;71:245–54.
22. Gendoo DM, Ratanasirigulchai N, Schroder MS, Pare L, Parker JS, Prat A, et al. Genefu: an R/Bioconductor package for computation of gene expression-based signatures in breast cancer. Bioinformatics 2016;32: 1097–9.
23. Jezequel P, Frenel JS, Campion L, Guerin-Charbonnel C, Gouraud W, Ricolleau G, et al. bc-GenExMiner 3.0: new mining module computes breast cancer gene expression correlation analyses. Database (Oxford) 2013;2013:bas060.
24. Samanta D, Gilkes DM, Chaturvedi P, Xiang L, Semenza GL. Hypoxia-inducible factors are required for chemotherapy resistance of breast cancer stem cells. Proc Natl Acad Sci U S A 2014;111:E5429–38.
25. Synnestvedt K, Furuta GT, Comerford KM, Louis N, Karhausen J, Eltzschig HK, et al. Ecto-5'-nucleotidase (CD73) regulation by hypoxia-inducible factor-1 mediates permeability changes in intestinal epithelia. J Clin Invest 2002;110:993–1002.
26. Derynck R, Muthusamy BP, Saeteurn KY. Signaling pathway cooperation in TGF-beta-induced epithelial-mesenchymal transition. Curr Opin Cell Biol 2014;31:56–66.
27. Hatfield SM, Sitkovsky M. A2A adenosine receptor antagonists to weaken the hypoxia-HIF-1alpha driven immunosuppression and improve immunotherapies of cancer. Curr Opin Pharmacol 2016;29:90–6.
28. Wang H, Lee S, Nigro CL, Lattanzio L, Merlano M, Monteverde M, et al. NT5E (CD73) is epigenetically regulated in malignant melanoma and associated with metastatic site specificity. Br J Cancer 2012;106:1446–52.
29. Lo Nigro C, Monteverde M, Lee S, Lattanzio L, Vivenza D, Comino A, et al. NT5E CpG island methylation is a favourable breast cancer biomarker. Br J Cancer 2012;107:75–83.
30. Spychala J, Lazarowski E, Ostapkowicz A, Ayscue LH, Jin A, Mitchell BS. Role of estrogen receptor in the regulation of ecto-5'-nucleotidase and adenosine in breast cancer. Clin Cancer Res 2004;10:708–17.
31. Wu Y, Ginther C, Kim J, Mosher N, Chung S, Slamon D, et al. Expression of Wnt3 activates Wnt/beta-catenin pathway and promotes EMT-like phenotype in trastuzumab-resistant HER2-overexpressing breast cancer cells. Mol Cancer Res 2012;10:1597–606.
32. Oliveras-Ferraros C, Corominas-Faja B, Cufi S, Vazquez-Martin A, Martin-Castillo B, Iglesias JM, et al. Epithelial-to-mesenchymal transition (EMT) confers primary resistance to trastuzumab (Herceptin). Cell Cycle 2012;11:4020–32.
33. Miller LD, Chou JA, Black MA, Print C, Chifman J, Alistar A, et al. Immunogenic subtypes of breast cancer delineated by gene classifiers of immune responsiveness. Cancer Immunol Res 2016;4:600–10.
34. Cox TR, Rumney RM, Schoof EM, Perryman L, Hoye AM, Agrawal A, et al. The hypoxic cancer secretome induces pre-metastatic bone lesions through lysyl oxidase. Nature 2015;522:106–10.
35. Pankova D, Chen Y, Terajima M, Schliekelman MJ, Baird BN, Fahrenholtz M, et al. Cancer-associated fibroblasts induce a collagen cross-link switch in tumor stroma. Mol Cancer Res 2016;14:287–95.
36. Ju JA, Godet I, Ye IC, Byun J, Jayatilaka H, Lee SJ, et al. Hypoxia selectively enhances integrin receptor expression to promote metastasis. Mol Cancer Res 2017;15:723–734.
37. Nannuru KC, Futakuchi M, Varney ML, Vincent TM, Marcusson EG, Singh RK. Matrix metalloproteinase (MMP)-13 regulates mammary tumor-induced osteolysis by activating MMP9 and transforming growth factor-beta signaling at the tumor-bone interface. Cancer Res 2010; 70:3494–504.
38. Schultz-Cherry S, Lawler J, Murphy-Ullrich JE. The type 1 repeats of thrombospondin 1 activate latent transforming growth factor-beta. J Biol Chem 1994;269:26783–8.
39. Wang Z, Xiong S, Mao Y, Chen M, Ma X, Zhou X, et al. Periostin promotes immunosuppressive premetastatic niche formation to facilitate breast tumour metastasis. J Pathol 2016;239:484–95.
40. Wirsdorfer F, de Leve S, Cappuccini F, Eldh T, Meyer AV, Gau E, et al. Extracellular adenosine production by ecto-5'-Nucleotidase (CD73) enhances radiation-induced lung fibrosis. Cancer Res 2016; 76:3045–56.
41. Ambrosino E1, Spadaro M, Iezzi M, Curcio C, Forni G, Musiani P, Wei WZCavallo F Immunosurveillance of Erbb2 carcinogenesis in transgenic mice is concealed by a dominant regulatory T-cell self-tolerance. Cancer Res 2006;66:7734–40.
42. Hay CM, Sult E, Huang Q, Mulgrew K, Fuhrmann SR, McGlinchey KA, et al. Targeting CD73 in the tumor microenvironment with MEDI9447. Oncoimmunology 2016;5:e1208875.
43. Young A, Ngiow SF, Barkauskas DS, Sult E, Hay C, Blake SJ, et al. Co-inhibition of CD73 and A2AR adenosine signaling improves anti-tumor immune responses. Cancer Cell 2016;30:391–403.

Cancer Research
The Journal of Cancer Research (1916–1930) | The American Journal of Cancer (1931–1940)

AACR American Association for Cancer Research

CD73 Promotes Resistance to HER2/ErbB2 Antibody Therapy

Martin Turcotte, David Allard, Deepak Mittal, et al.

Cancer Res 2017;77:5652-5663. Published OnlineFirst August 30, 2017.